Journal of Engineering and Applied Research (JEAR)

Technical and Vocational University

Winter & Spring 2024, Vol. 1, No. 1, p. 93-110

Journal Homepage: https://jear.tvu.ac.ir/

:10.48301/JEAR.2024.191697

TVU

Making a Laboratory Sample of a Rotary Dehumidifier Wheel with a Focus on Making the base Material of the Wheel

Mostafa Hosseinalipour[1], Milad Esfandiar[2], Avishan Parkhideh[3*]

[1]Professor of Mechanical Engineering, Head of Energy, Water and Environment Research Center; Tehran, Iran.
[2]Faculty Member, Department of Mechanical Engineering Technical Vocational University (TVU) Tehran, Iran.
[3]Mechanical Department of Iran University of Science and Technology, Tehran, Iran.

ARTICLE INFO

Article Type:
Original Research

Received: 12.17.2023
Revised: 02.12.2024
Accepted: 03.03.2024

Keyword:
Desiccant
Sustainable Technology
Cooling
Technical Review
Dehumidification

***Corresponding Author:**
Avishan Parkhideh
Email:
avi.parkhideh@gmail.com

ABSTRACT

The desiccant wheel system is a topic of research because of increased requirements in the HVAC industry and dehumidification industry. Heat and mass transfer to remove water or other solvents is called the drying process. By passing air over solid, semi-solid and liquid materials, humidity can be reduced. Air conditioning is a process that collects the hot air of the desired environment, cools it with a refrigerant and then blows the cooled air into the desired environment. Using the desiccant process is the only cost-effective method. Solid dehumidifier absorbs water using chemical absorption. A number of solid desiccant samples include silica gel, natural zeolite, activated alumina and synthetic polymers. Desiccant is a hygrometer that is generally used as a drying agent in dryers and air conditioning systems. The function of the desiccant is to remove moisture from the air to reduce the humidity of the surrounding air for people's comfort. After the dehumidifier becomes saturated, it is put under the dehumidification process by passing hot air to revive it and make the process continuous. Like all air conditioning systems, this device also has its advantages and disadvantages. Its advantages include intermittent air drying with low energy consumption. Furthermore, its benefits include low capacity in moisture absorption and pressure reduction. Using this method affects the efficiency of the system and the desiccant must be cooled after complete drying.

E-ISSN: 3060-6357

Introduction

Desiccants play a crucial role in various applications by efficiently adsorbing moisture from the air. In the context of space conditioning, the effectiveness of desiccants lies in their capacity to retain significant quantities of water vapor without the need for cooling to the dew point, which can often lead to decreased energy efficiency. Common solid desiccants such as silica gel, molecular sieve, and activated alumina are known for their ability to hold water up to more than half of their weight.

Beery (2000) studied solid side resistance differently [1]. They solved the diffusion coefficient equation for moisture passage on the solid side, assuming a parabolic concentration profile (PCP) inside the constituent part. Based on the PCP model, Chant developed a heat and mass transfer model used for a desiccant wheel with moist laminar airflow. The experimental data matched with simulation results. Dai et al. (2001) obtained wave analysis to evaluate rotary desiccants' performance using a psychometric chart [2]. According to the wave, the shape was proposed to improve dehumidification performance and specific essential parameters such as heat capacity, rotation speed, adsorption heat, desiccant matrix thickness, regeneration temperature and desiccant isothermal shape which were deliberated in information using a psychrometric chart. Sharma and colleagues [3] provided a better understanding of the existing research and designs for dehumidifier wheel systems. The difference between liquid and solid dehumidifiers in cooling systems, different wheel regeneration technologies, the use of various drying materials, building design of the wheel in terms of the number of sections and the direction of airflow in the dryer were discussed. In this paper [4], the recent optimization techniques for rotary drying systems are summarized by Zhoa Du et al. Five aspects of optimization such as the new development of composite dryers, the invention of dryer bed structure, the new design of circulation system, increasing efficiency of low-grade source energy and optimal operation conditions with air conditioning are described. This review might be a reference for the actual application of the rotary screw dehumidification system. Chaudhary et al. [5] presented a real-time performance analysis of a silica gel dehumidifier wheel. The thermodynamic model was also validated through comparison under a wide range of operating conditions for subtropical climate conditions. First, a mathematical model was developed using a set of different equations for the dryer wheel in the Engineering Equation Calculator (EES). Second, a parametric analysis of this system including various design and climate parameters such as inlet air humidity ratio, inlet air temperature, relative humidity of regeneration air inlet, regeneration temperature and wheel rotation speed was conducted. Then, a trial run of the system was made in Taxila, Pakistan to evaluate

the real-time performance of the results and showed that the optimum rotation speed of the dryer wheel was between 15-17 rpm. The maximum effectiveness based on the mathematical and experimental model were 0.45 and 0.43 respectively at a reduction temperature of 80 °C. The maximum and minimum root mean square error (RMSE) for effectiveness were 3.2% and 2.1%, respectively. Therefore, the comparison between experimental and model results showed good agreement. Ortis and Khatiwada [6] performed a comparative life cycle assessment of two desiccant wheel dehumidifiers for industrial applications and identified the key influencing factors of selected environmental impact categories, such as climate change, ozone depletion, and fine particulate matter formation. Ashutosh Verma et al. [7] wrote an article on a one-dimensional mathematical model which was developed to analyze the parameters of the passive wheel and to compare it with the existing active desiccant wheel, which is a rotating dehumidifier that can be regenerated using the room's return (exhaust) air and does not require hot air for regeneration. Abdelgaied et al. [8] proposed an innovative design of a desiccant dehumidifier that had a higher dehumidification capacity in addition to cooling the process air with cooling rates higher than the heat generated by the adsorption effect. Wang et al. as discussed by Bowen Guan [9] proposed a novel air-conditioning system with cascading desiccant wheel and liquid dehumidifier for low-humidity industrial workshops, which achieved a supply air dew point temperature below −10 °C. Singh et al. [10] discussed the performance of a rotary desiccant wheel which was evaluated using a new set of independent efficacy metrics and a correlation between experimental and anticipated results was developed based on the experimental data. Vivekh et al. [11] researched a 3D mathematical model that was developed to study the time-dependent and steady-state temperature, humidity, and reaction distributions of desiccant wheel dehumidifiers. Liu et al. [12] studied a one-dimensional gas-side resistance model employed to mimic a silica gel desiccant wheel, and one of the state-of-the-art policy gradient algorithms, proximal policy optimization (PPO), was utilized to train a feedback controller for this AC system. Prasad et al. [13] studied an experimental setup integrated with calcium chloride (CaCl2)-based rotating desiccant material and solar heating arrangement to make the system eco-friendly; the experimental finding of the current study was also validated with a mathematical model. Liu et al. [14] studied a metal-organic framework composite adsorbent desiccant wheel (MOF DW) prepared by the impregnating-spraying method, and the complete rotary wheel dehumidification system was built to compare the dehumidifying performance of MOF DW and commercial silica gel desiccants wheel (SG DW). Yang et al. [15] studied an ICP system which was developed to refine aluminium hydroxide extracted from aluminium residues into

activated alumina by utilizing its high energy densities, and a six-turn induction coil was suitable for the present study matchbox to produce an alternating electromagnetic field to sustain space discharge, and to have well reaction zone.

This paper explores advancements in desiccant-based dehumidification and cooling systems. Specifically, it focuses on a novel approach involving changes in the placement of absorbent layers within the moisture-absorbing wheel. Unlike traditional designs where absorbent layers are parallel to the airflow, the innovation of the present research lies in arranging the layers perpendicular to the flow. Additionally, a combined absorbent material comprising sodium silicate and aluminium sulfate, departing from conventional choices such as silica gel and zeolite, was utilized.

In the following sections, the theoretical underpinnings of the present study approach, drawing on previous research are investigated. The experimental findings that demonstrate the efficacy of the modified desiccant wheel design are also presented. The potential benefits and practical applications of this innovative approach in improving dehumidification and cooling systems are highlighted through a comprehensive analysis.

Mathematical model of the desiccant wheel

The mathematical model of the desiccant wheel was based on various sets of algebraic equations for determining absolute humidity and temperature on the process as well as the regeneration side. Furthermore, additional correlations were also used to find moist air-specific properties under a wide range of operating conditions such as specific enthalpy to temperature, and relative humidity to humidity ratio. The total amount of moisture adsorbed in the desiccant wheel was determined through adsorption isotherms [16]. Adsorption material strongly influences these isotherms in addition to inlet humidity [17; 18]. Adsorption isotherms characterize the amount of water absorbed by the desiccant wheel and depend upon adsorbent material. Therefore, to determine the equilibrium amount of moisture adsorbed (q_{eq}) as a function of relative humidity, Freundlich Equation (1) was used.

$$q_{eq} = C(RH)_{in}^{\frac{1}{n}} \tag{1}$$

The isosteric heat of adsorption was found by using the Clausius–Clapeyron relationship, whose range was between 2100 and 2300 kJ/kg. The surface diffusivity was linked to temperature via the Arrhenius Equation (2) which is used to calculate the activation energy for diffusion. This activation energy is approximately 80% of the isosteric heat of adsorption and offers a good realistic estimate [19].

$$D_{sf} = 2.27 * 10^{-7} exp\left[\frac{E_{at}}{R\left(\frac{T_{\{sin\}} + T_{\{reg\}}}{2}\right)}\right] \quad (2)$$

Additionally, sensible heat exchange between the process and regeneration side through wheel rotation per unit time was determined by Equation (3) [18].

$$H_1 = \frac{\rho_{dw} C_{pc}\left(T_{reg} - T_{\{sin\}}\right) NL}{\beta_s \rho_a U_s} \quad (3)$$

The majority of mathematical models for desiccant wheels can be categorized into two types.

1- The model that considers the heat and mass transfer resistance offered by the bulk gas, while ignoring the resistance offered by the solid material of the wheel.
2- The model that considers both resistances such as solid side and bulk gas molecules

The current model was modified to calculate the mass transfer by considering surface diffusion as the dominant factor. Therefore, the amount of water vapor adsorbed by the adsorbent material is given by Equation (4).

$$q = 1.129\sqrt{D_{sf} t_1 \rho_{ad}}\rho_{ad} A_{ws} q_{eq} \quad (4)$$

Here t1 is the adsorption time which is computed by $t_1 = \frac{3600 B_s}{N_w}$. Subsequently, hourly measurements of water exchange from process air to the regeneration air through the desiccant wheel were determined by Equation (5).

$$Q_m = qSL\rho_{dw} N \quad (5)$$

The conditions at the outlet of the process and regeneration stream depend upon heat and mass transfer as given in equations (3), and (5). The absolute humidity ratio on the process outlet side was calculated by Equation (6).

$$W_{sout} = W_{\{sin\}} - \frac{Q_m}{m_s} \quad (6)$$

Where m_s is the mass flow rate of process air and is determined by Equation (7).

$$m_s = \rho_a U_s S \tag{7}$$

The enthalpy and temperature of the process air at the outlet were determined using Equations (8) and (9).

$$h_{sout} = h_{\{sin\}} + H_1 \tag{8}$$

$$T_{sout} = \frac{h_{sout} - 2501 W_{sout}}{1.86 W_{sout} + 1.006} + 273.15 \tag{9}$$

The dehumidification effectiveness of the desiccant wheel was defined as the ratio of dehumidification achieved from the desiccant wheel to the inlet humidity when the ideal humidity at the outlet is considered to be zero. The parameter is given as Equation (10) [20].

$$\varepsilon_d = \frac{w_{\{sin\}} - w_{sout}}{w_{sout} - w_{ideal}} \tag{10}$$

where W_{ideal} is the specific humidity of the air at the desiccant wheel outlet. If its value is considered to be zero it will represent an ideal wheel that will completely dehumidify the air. The present study model is modular and is flexible to adopt different values of design parameters.

Model of desiccant wall

In this section, the governing equations inside the desiccant wall are discussed. The governing equations were developed based on some assumptions. The main assumptions were as follows [21]:

1- The partial density of the dry air in the pore is constant.
2- Inside the desiccant wall, the temperature and concentration distribution in the wall thickness direction (y) and the channel length direction (z) are considered (two dimensions), i.e.

Ta = Ta(t, y, z), wa = wa(t, y, z), Td = Td(t, y, z), xd = xd(t, y, z).

3- The desiccant wall is a homogeneous material.
4- The transfer of the water vapor is caused only by the diffusion, i.e. the transfer by the convection is ignored.
5- The pore diffusion is the unidirectional diffusion of the water vapor.

6- The temperature and concentration of the humid air in the pore are locally in equilibrium with those of the adsorbed water on the solid surface at the same place.
7- The temperature dependence and adsorption–desorption hysteresis of the adsorption isotherm is ignored because those of the sodium silicate is small.

The desiccant wall is porous solid. The governing equations are developed by considering the heat and mass diffusion inside the porous solid. The mass diffusion equation of the water vapor in the pore is as follows:

$$\varepsilon \frac{\partial}{\partial t}(\rho_a w_a) + \nabla . j_p = \dot{m} \tag{11}$$

where $\boldsymbol{\dot{m}}$ is the amount of desorbed water per unit volume from the solid surface to the pore. J_p is the mass flux caused by the pore diffusion and is given by

$$j_p = -\frac{\varepsilon D_p}{\tau_p} \nabla(\rho_a w_a) \tag{12}$$

The mass diffusion equation of the adsorbed water on the solid surface is as follows:

$$(1-\varepsilon) \frac{\partial}{\partial t}(\rho_d \omega_d) + \nabla . j_s = \dot{m} \tag{13}$$

where js is the mass flux caused by the surface diffusion and is given by:

$$j_s = -\frac{(1-\varepsilon) D_s}{\tau_s} \nabla(\rho_d \omega_d) \tag{14}$$

Because the continuum and Knudsen diffusions are considered to occur in series, the pore diffusivity is expressed as follows:

$$\frac{1}{D_p} = \frac{1}{D_m} + \frac{1}{D_K} \tag{15}$$

Sherwood et al. [22] proposed the following expression as the continuum diffusivity of the water vapor in the humid air.

$$D_m = \frac{0.926 \times 10^{-3}}{P_t} \left(\frac{T_a^{2.5}}{T_a + 245} \right) \tag{16}$$

Kennard [23] proposed the following expression as Knudsen diffusivity in the pore whose mean pore radius is γ.

$$D_k = 97\gamma\left(\frac{T_a}{M_w}\right)^{1/2} \quad (17)$$

Gilliland et al. [24] proposed the following expression as the surface diffusivity:

$$D_s = 1.6 \times 10^{-6}\, exp\left(-0.45\,\frac{h_{ads}}{R_w T_d}\right) \quad (18)$$

Inside the desiccant wall, as mentioned above, three different diffusions occur. Concretely, the continuum diffusion and Knudsen diffusion occur in series in the pore and these two diffusions are summarized as the pore diffusion. Moreover, the pore diffusion and the surface diffusion are considered to occur in parallel. Under the condition of this study, surface diffusion is dominant among the different diffusions in the desiccant wall.

Production stages

1- Use of stainless-steel mesh as shown in Figure (1).
2- Contact the base material (stainless steel mesh) with a neutral sodium-grade silicate solution with a concentration of 15 to 40 per cent with or without activated carbon. In the manufacture of adsorbents, unlike the adsorbents mentioned in previous sections, it could be harder to choose moisture adsorbents; but neutral sodium-grade silicate was used because after combining with aluminium sulfate or magnesium sulfate, it will have high moisture adsorption properties. It should be noted that silica gel is also made of the same material, but the reason for not using silica gel as an absorbent material was that after heating this material inside the silica gel furnace, it will be separated from the base material in powder form and will cause problems with coating operations.
3- Drying and delivering moisture to approximately 15 to 40 percent as shown in Figure (2).
4- Submersion of the dried plate in the previous stage in a solution of metal salts such as aluminium sulfate, magnesium sulfate, magnesium chloride and aluminium chloride, or weak acid such as phosphoric acid to form hydrogels, at which point it is necessary to control concentrations, temperature and coating time.
5- Washing with water to remove excess material from the pieces (pH control of washing).

6- Drying with a hot air blower like a hair dryer.
7- Measuring the temperature of the piece to prevent a sudden temperature rise.

Figure 1. Open-cell aluminium foam.

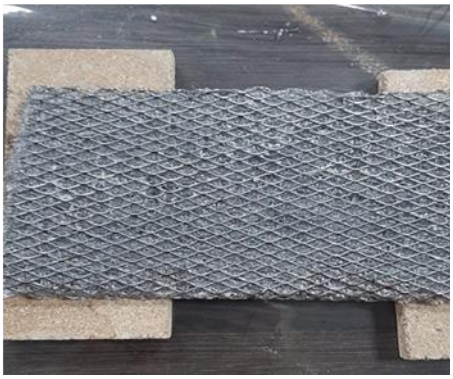

Figure 2. Coated stainless steel grille with Silicate glue.

Reactions that occur during the process:

$$Na2SiO3 + HCl \rightarrow H2SiO3 + NaCl$$

$$Na2SiO3 + AlCl3 \rightarrow Al2(SiO3)3 + NaCl$$

$$Na2SiO3 + MgCl2 \rightarrow MgSiO3 + NaCl$$

$$Na2SiO3 + MgSO4 \rightarrow MgSiO3 + Na2SO4$$

$$Na2SiO3 + Al2(SO4)3 \rightarrow Al2(SiO3)3 + Na2SO4$$

Making a second sample

To make a second sample to examine the idea of the perpendicular layers of absorbent, SOLIDWORKS software was used to design the prototype of the wheel layers in a sinusoidal manner as shown in Figures (3) and (4) and to maintain the sinusoidal flow between the layers, the seams were filled with aquarium glue.

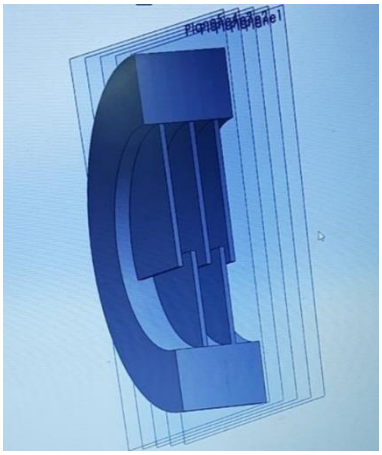

Figure 3. Side section view of the sinusoidal structure of the wheel.

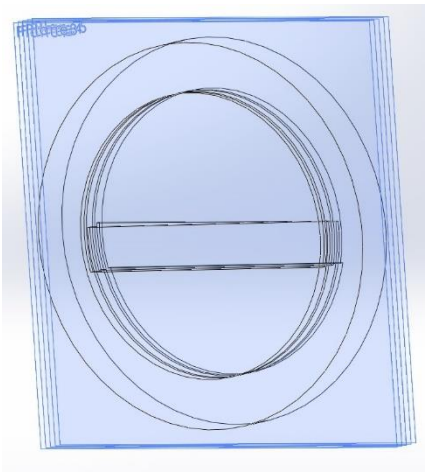

Figure 4. Complete view of the sinusoidal structure of the wheel.

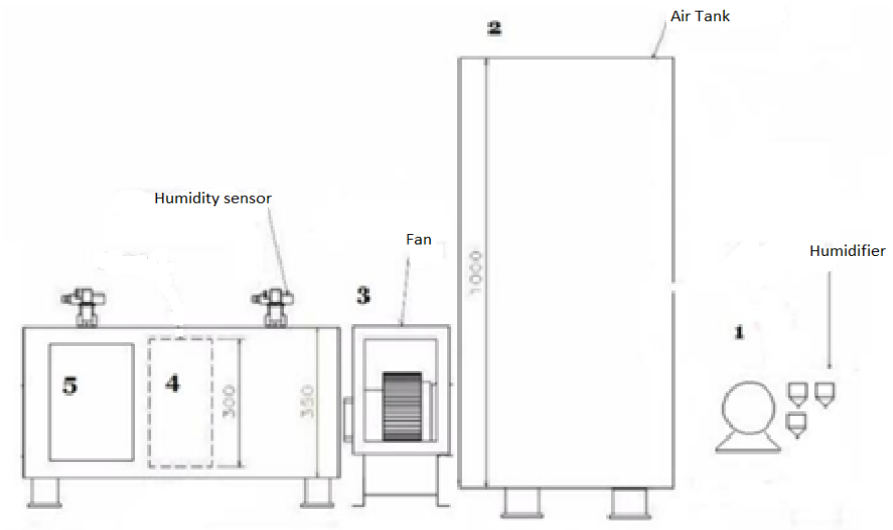

Figure 5. Schematic of package component.

Laboratory setup

As shown in Figure (6), a system which was built by Mr Hosseinalipour et al. for his research [25] was used after optimizing the system. In addition, Figure (5) shows the schematic of the package component which was designed by Mr. Hosseinalipour et al.

1- Moisture source
2- Wet air storage compartment
3- Supply and fan air intake chamber

4- Laboratory sample
5- Supply air outlet and recovery air inlet

Figure 6. Setup of the system used.

Test and result analysis

The test involved the supply air intake fan speed, the rotational speed of the moisture-absorbing wheel, and the recovery heat temperature; these parameters can be considered constant and variable according to the conditions of the test. According to the above, the fan built into the system had a maximum circumference of 1250 rpm and a minimum circumference of 200 rpm. In the first stage, two other parameters were designed to be constant, where the fan circumference varied by 200, 400, 600 and 800 rpm. The test was conducted so that the pump, fan and heater were put on and moisture was measured when moisture was added from the tank containing distilled water into the humid air collection tank. After reaching the stable conditions, the number indicated in the humidity sensor was recorded, followed by a measurement of the amount of moisture in the incoming air after the fan suction. Because the distillation process was performed and the humidity decreased in the distance between the outlet nozzle of the wet air and the distillation fan, the moisture loss rate was also measured at the wheel entrance after reaching stable conditions. Then, the air moisture was examined after passing through the moisture-absorbing wheel. It should be noted that all tests were performed after the conditions had reached a stable state. The steps and results of the tests carried out in the first part are as follows:

Table 1. Measuring temperature and humidity in the parallel layers.

Wheel velocity (RPM/min)	Fan velocity (RPM/min)	Source humidity	Incoming and outgoing humidity difference	Average output humidity	Average input humidity	Average output temp. ℃	Average input temp. ℃
6	200	100%	22.2%	43.5%	65.7%	22.2	21.4
6	300	100%	12.45%	39.2%	50.34%	23.3	22.5
6	400	100%	11.37%	32.5%	43.87%	23.4	22.97
6	500	100%	11.21%	31.9%	44.4%	23.6	23.1
6	600	100%	10.98%	34.9%	45.67%	23.9	23.5
6	700	100%	9.78%	37.8%	46.59%	24.1	23.4
6	800	100%	9.34%	40.97%	47.5%	24.4	22.84

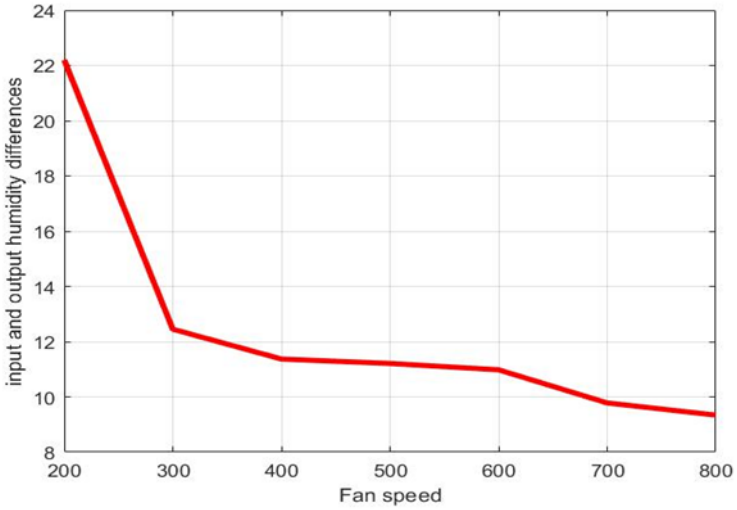

Figure 7. Examination of input and output humidity differences based on fan speed.

As shown in Table (1), when the fan circumference in the incoming airflow is 200 rpm, the moisture absorption rate is higher once the absorbent layers are parallel to the current. In this case, the humidity of the air decreases from 65%, which is measured at a point before the wheel, to 43%, which is considered a desirable result compared to similar laboratory samples with almost the same efficiency. According to the temperature measurement before and after the absorption process, it was observed that despite the heat of the process, the temperature of the exhaust air had not increased significantly. Figure (7) corresponding to the data shows that the moisture absorption rate decreased with the increase in the fan circumference.

Another comparison shows that as the temperature rises, the moisture decline process begins. It can be concluded that this is due to the low temperature; the

process of reviving the wheel slows down and the absorption efficiency decreases, and with an increase in the humidity of the wheel during dehumidification and the lack of revival, the dehumidification capacity of the absorbent materials decreases, leading to a decrease in efficiency.

The next step was to measure the percentage of moisture absorption by keeping the fan circumference constant and the variability of the rotation speed of the absorbent wheel. In the second stage, the fan rotation was selected as a constant parameter at a speed of 800 rpm, and the variable speeds of 3, 6 and 12 RPM were considered for the rotation of the monetary system and the belt. It is noteworthy that in the first series of tests, the speed of dehumidifying the wheel was consistently 6 rpm. The results of the second series of tests in Table (2) are as follows:

Table 2. Measuring temperature and humidity in parallel layers.

Wheel velocity (RPM/min)	Fan velocity (RPM/min)	Source humidity	Incoming and outgoing humidity difference	Average outgoing humidity	Average incoming humidity	Average output temp. ℃	Average input temp. ℃
3	800	100%	24.56%	54.54%	79.1%	23.1	22.4
6	800	100%	29.37%	48.6%	77.97%	23.8	22.74
12	800	100%	22.03%	42.57%	64.6%	24.3	23.77

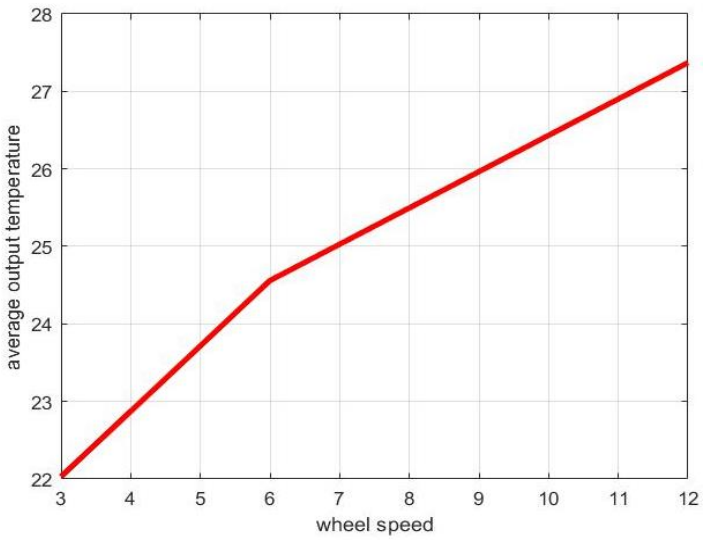

Figure 8. Examination of input and output humidity differences based on fan speed.

According to Table (2), the best round of the wheel, which had the highest moisture absorption, was 6 rpm. As shown in Figure (8), unlike the fan cycle, in which a decrease in efficiency was observed, the adjustments related to the

rotation of the absorbent wheel with the increase in the speed of the wheel, the amount of moisture absorption was higher than the lower speed of the wheel. With an increase in the speed of the fan cycle, the input to the system also increased. It can be concluded that increasing the input discharge until the dehumidification capacity is reduced will be useful and the system efficiency can be improved by controlling the input discharge and preventing its efficiency from decreasing. The effect of pressure drops in the tests performed was ignored due to the small pressure difference. As mentioned, the study was focused on improving and supplementing the system in the Water, Energy and Environmental Laboratory, so the moisture removal capacity of the system was calculated and the ratio of previous tests on the system was measured.

In the third part of the experiment, the wheel with absorbent layers made perpendicular to the current was examined. This section compares the absorption rate of moisture using the change of the incoming air fan circumference. As can be seen in Table (3), on average, the percentage of moisture absorption increased with the increase in fan speed, so at 800 RPM, the highest percentage of moisture absorption, 23.34%, was observed. This was unlike the previous experiment, where the increase in temperature led to an increase in moisture absorption.

Table 3. Comparison of moisture absorption at different velocities of the input fan when the layers are perpendicular to the flow.

Wheel velocity (RPM/min)	Fan velocity (RPM/min)	Source humidity	Incoming and outgoing humidity difference	Average outgoing humidity	Average incoming humidity	Average output temp. ℃	Average input temp. ℃
6	200	100%	23.1%	42.5%	63%	27.1	27.04
6	300	100%	23.17%	42.17%	65.34%	27.17	27.1
6	400	100%	23.19%	41.45%	64.64%	27.2	27.2
6	500	100%	23.24%	41.01%	64.25%	27.24	27.2
6	600	100%	23.26%	39.8%	63.04%	27.43	27.34
6	700	100%	23.29%	39.56%	62.15%	27.45	27.3
6	800	100%	23.34%	39.2%	61.54%	27.49	27.3

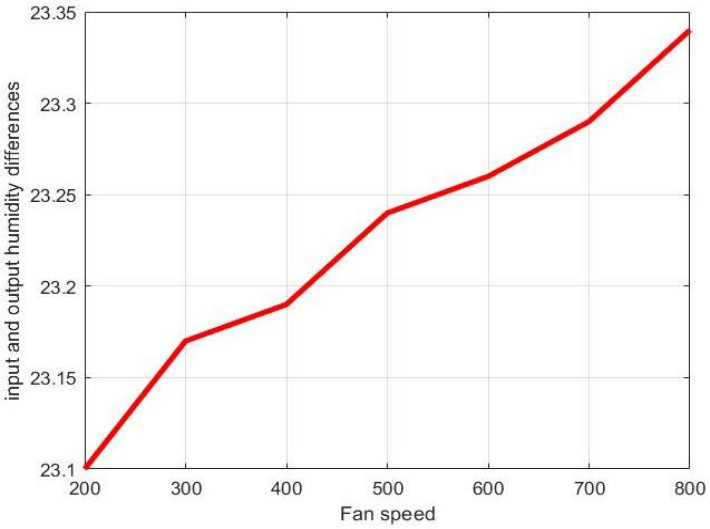

Figure 9. Examination of output temperature differences based on fan speed.

The next step was to measure the percentage of moisture absorption when the absorbent layers were perpendicular to the current by keeping the fan circumference constant and the speed of the absorbent wheel rotation variable. In this process, the fan circumference was maintained constant at 800 revolutions per minute because the best speed for absorbing moisture was known in the previous experiment. In this series of tests, as can be observed in Table (4) and shown in Figure (9), the rate of moisture absorption decreased with the speed of the wheel due to the wheel not having much time to go through the regeneration process, thereby decreasing its absorption power. In another comparison, despite the increase in temperature, the rate of moisture absorption did not increase, and as mentioned, due to the high speed of the wheel, the opportunity to regenerate the wheel decreases and so the temperature increase is inefficient.

Table 4. Comparison of moisture absorption at different speeds of the absorbent wheel when the layers are perpendicular to the flow

Wheel velocity (RPM/min)	Fan velocity (RPM/min)	Source humidity	Incoming and outgoing humidity difference	Average output humidity	Average input humidity	Average output temp. ℃	Average input temp. ℃
3	800	100%	24.33%	37.04%	61.37%	27.7	27.54
6	800	100%	22.13%	36.67%	58.8%	28.1	27.94
12	800	100%	19.4%	36.6%	56%	28.2	28

Discussion

Based on the recorded amounts of moisture absorption in the wheel made of stainless-steel mesh base material and sodium silicate and aluminium sulfate absorbent material, it was concluded that if the wheel core is such that the absorbent layers are perpendicular to the current, in addition to the higher absorption percentage, the output temperature increases by a small amount. In this study, the best absorption conditions were reported for 800 rpm, 23 ° C process temperature and 3 RPM perpendicular to the current.

Conclusion

In the construction of rotary dehumidification systems, the use of experiences and articles published by other manufacturers of these systems in developed countries is a good roadmap for its domestic production. The stainless-steel mesh was used due to the lack of access to open-cell aluminium foam, which, although not expected to form a suitable porous environment, enabled the appropriate moisture absorption rate. In the manufacture of rotary dehumidifiers, the use of sodium silicate absorbent with aluminium sulfate as a base material in the manufacture of silica gel created a moisture absorption capacity of up to 25% relative humidity. In metal mesh coating operations, the metal mesh absorbent compound was used to absorb the moisture-absorbent material as much as the mass weight of the material itself, which in itself expresses the high quality of the synthesis coating operations. In the construction of a laboratory sample, it is possible to achieve the desired amount of moisture absorption (31% relative humidity) by precisely controlling the flow parameters such as the speed and flow rate of the input to the system, the rotational speed of the absorbent wheel, as well as the process temperature.

Disclosure statement and funding

The authors declare no potential conflicts of interest. The present study received no financial support from any organization or institution.

Acknowledgment

We would like to give special thanks to all the participants in this study.

References

[1] Beery, K. E. (2000). *Characterization of a starch based desiccant wheel dehumidifier* [Doctoral, Purdue University]. West Lafayette, Indiana. https://www.proquest.com/openview/e1d994555778c8c5b02fbe3b9df75892/1?pq-origsite=gscholar&cbl=18750&diss=y

[2] Dai, Y. J., Wang, R. Z., & Zhang, H. F. (2001). Parameter analysis to improve rotary desiccant dehumidification using a mathematical model. *International Journal of*

Thermal Sciences, *40*(4), 400-408. https://doi.org/10.1016/S1290-0729(01)01224-8

[3] Sharma, A., Mishra, S. K., Verma, A. K., & Yadav, L. (2022, May 26-28). *A technical review of available desiccant design techniques.* International Conference on Advances in Mechanical Engineering-2022, Nagpur, India. https://doi.org/10.1088/1757-899X/1 259/1/012004

[4] Du, Z., & Lin, X. (2020, April 10-12). *Research Progress of Rotary Desiccant Wheel Optimization Technology.* 4th International Workshop on Advances in Energy Science and Environment Engineering, Hangzhou, China. https://doi.org/10.1088/1755-131 5/512/1/012181

[5] Chaudhary, G. Q., Ali, M., Ashiq, M., Ali, H. M., & Amber, K. P. (2019). Experimental and model based performance investigation of a solid desiccant wheel dehumidifier in subtropical climate. *Thermal Science*, *23*(2), 975-988. https://doi.org/10.2298/TS CI170127165C

[6] Ortis, A., & Khatiwada, D. (2023). A comparative life cycle assessment of two desiccant wheel dehumidifiers for industrial applications. *Energy Conversion and Management*, *286*, 117058. https://doi.org/10.1016/j.enconman.2023.117058

[7] Verma, A. K., Yadav, L., Kumar, N., & Yadav, A. (2023). Mathematical investigation of different parameters of the passive desiccant wheel. *Numerical Heat Transfer, Part A: Applications*, *84*(10), 1149-1168. https://doi.org/10.1080/10407782.2023.2172491

[8] Abdelgaied, M., Saber, M. A., Bassuoni, M. M., & Khaira, A. M. (2023). Comparative analysis of a new desiccant dehumidifier design with a traditional rotary desiccant wheel for air conditioning purpose. *Applied Thermal Engineering*, *222*, 119945. https://doi.or g/10.1016/j.applthermaleng.2022.119945

[9] Guan, B., Ma, Z., Wang, X., Liu, X., & Zhang, T. (2022). A novel air-conditioning system with cascading desiccant wheel and liquid desiccant dehumidifier for low-humidity industrial environments. *Energy and Buildings*, *274*, 112455. https://doi.org/10.101 6/j.enbuild.2022.112455

[10] Singh, R. P., Das, R. K., & Upadhyay, N. (2023). Effectiveness approach for predicting desiccant wheel performance: correlation utilizing experimental results. *International Journal of Refrigeration*, *156*, 84-91. https://doi.org/10.1016/j.ijrefrig.2022.11.016

[11] Vivekh, P., Pei, S. D., Pang, W., & Cheng, G. (2023). Air dehumidification performance study of a desiccant wheel by a three-dimensional mathematical model. *International Journal of Refrigeration*, *147*, 163-173. https://doi.org/10.1016/j.ijrefrig.2022.10.011

[12] Liu, J., Jiang, C., Li, X., & Zhang, W. (2022, July 25-27). *Deep reinforcement learning for the control of a desiccant wheel-based air-conditioning system.* 41st Chinese Control Conference Hefei, China. https://doi.org/10.23919/CCC55666.2022.9901521

[13] Prasad, A. K., Singh, D. K., & Shankar, R. (2022). Performance analysis of heating and humidification system with solar assisted CaCl2 desiccant wheel rotor. *Energy Sources, Part A: Recovery, Utilization, and Environmental Effects*, *44*(4), 9086-9102. https:// doi.org/10.1080/15567036.2022.2128941

[14] Liu, Z., Cheng, C., Han, J., Zhao, Z., & Qi, X. (2022). Experimental evaluation of the dehumidification performance of a metal organic framework desiccant wheel.

International Journal of Refrigeration, *133*, 157-164. https://doi.org/10.1016/j.ijrefrig.2021.09.033

[15] Yang, S. F., Wang, T. M., Chen, C. L., Lee, H. M., Li, H. Y., & Huang, S. W. (2021). Porous Desiccant Wheel Produced Using Inductively Coupled Plasma Technique. *Institute of Electrical and Electronics Engineers Transactions on Plasma Science*, *49*(1), 177-181. https://doi.org/10.1109/TPS.2020.3003650

[16] Ali, M., Vukovic, V., Sahir, M. H., & Basciotti, D. (2013). Development and validation of a desiccant wheel model calibrated under transient operating conditions. *Applied Thermal Engineering*, *61*(2), 469-480. https://doi.org/10.1016/j.applthermaleng.20 13.08.010

[17] Ashrae Handbook Committee. (1996). *Heating, Ventilating, and Air-Conditioning Systems and Equipment systems and equipment*. American Society of Heating, Refrigerating and Air-Conditioning Engineers. https://iifiir.org/en/fridoc/1996-ashrae-handbook-hvac-systems-and-equipment-si-edition-1630

[18] Kodama, A., Goto, M., Hirose, T., & Kuma, T. (1995). Performance Evaluation for a Thermal Swing Honeycomb Rotor Adsorber Operated with Thermal Swing. *Journal of Chemical Engineering of Japan*, *28*(1), 19-24. https://doi.org/10.1252/JCEJ.28.19

[19] Kodama, A., Hirayama, T., Goto, M., Hirose, T., & Critoph, R. E. (2001). The use of psychrometric charts for the optimisation of a thermal swing desiccant wheel. *Applied Thermal Engineering*, *21*(16), 1657-1674. https://doi.org/10.1016/S1359-4311(01) 00032-1

[20] Mandegari, M. A., & Pahlavanzadeh, H. (2009). Introduction of a new definition for effectiveness of desiccant wheels. *Energy*, *34*(6), 797-803. https://doi.org/10.1016/j. energy.2009.03.001

[21] Yamaguchi, S., & Saito, K. (2013). Numerical and experimental performance analysis of rotary desiccant wheels. *International Journal of Heat and Mass Transfer*, *60*(1), 51-60. https://doi.org/10.1016/j.ijheatmasstransfer.2012.12.036

[22] Sherwood, T. K., & Pigford, R. L. (1952). *Absorption and Extraction* (2 ed.). McGraw-Hill. https://search.worldcat.org/title/Absorption-and-extraction/oclc/567332

[23] Kennard, E. H. (1938). *Kinetic Theory of Gases, with an Introduction to Statistical Mechanics*. McGraw-Hill. https://books.google.com/books?id=Wt5AAAAAIAAJ

[24] Gilliland, E. R., Baddour, R. F., Perkinson, G. P., & Sladek, K. J. (1974). Diffusion on Surfaces. I. Effect of Concentration on the Diffusivity of Physically Adsorbed Gases. *Industrial & Engineering Chemistry Fundamentals*, *13*(2), 95-100. https://doi.org/1 0.1021/i160050a001

[25] Hosseinalipour, S., Doodi, S., & Hosseini, S. M. (2023). Experimental Study Of Desiccant Dehumidifier System With Focus On Wheel Base Material. *Journal of Multidisciplinary Engineering Science and Technology*, *10*(4), 15905-15909. http://www.jmest.org/w p-content/uploads/JMESTN42354180.pdf